Eur. Phys. J. AP **17**, 209–214 (2002)
DOI: 10.1051/epjap:2002014

THE EUROPEAN PHYSICAL JOURNAL APPLIED PHYSICS

Investigation of deposition parameters and output functions, and production of low coercivity films

H. Kockar[1,a] and T. Meydan[2,b]

[1] Balikesir University, Science & Literature Faculty, Physics Department, Balikesir, 10100, Turkey
[2] Cardiff University, Wolfson Centre, Newport Road, PO Box 925, Cardiff, CF24 OYF, UK

Received: 15 March 2001 / Received in final form: 31 October 2001 / Accepted: 10 January 2002

Abstract. The correlation of deposition parameters with output functions when using a novel rotating cryostat (RC) system to produce magnetic materials has been investigated here. In order to do this, an orthogonal design technique was applied for magnetic material production using a resistively heated furnace. The results of orthogonal analysis indicate that the thickness uniformity across the film was not greatly improved, due to the large standard deviation, but an optimum deposition rate was obtained by appropriate choice of control parameters. Furthermore, the orthogonal design process was applied to systematically optimise the production of low coercivity in iron films. The results indicate that the process can be easily optimised.

PACS. 81.15.Ef Vacuum deposition – 81.15.Aa Theory and models of film growth – 75.50.Bb Fe and its alloys

1 Introduction

Magnetic thin film and multilayer science has now developed into major industries including the sensors and magnetic media sectors. This growth has occurred partly through improvements in the fundamental understanding of magnetic film behaviour and developments in thin film processing. For example high performance magnetic heads utilising soft magnetic thin films along with continuous developments in magnetic media is leading to rapid increases in magnetic recording densities. To improve the properties of magnetic materials careful control of input parameters is necessary during deposition. This has been demonstrated in this study by investigating the influence of input parameters on the coercivity in iron films.

A novel rotating cryostat (RC) system previously [1] used to prepare organic layers has been developed to produce magnetic materials. The main features of this system is its high speed rotating (up to 2000 rpm) liquid nitrogen cooled cylindrical drum 80 cm^2 (2 cm wide), and multiple evaporation sources see Figure 1. The aim of this extensive investigation was to deposit thin iron films using a resistively heated furnace in order to systematically evaluate the deposition process and parameters, and their corresponding output functions for producing low film coercivities. Orthogonal design technique was applied for process optimisation of film deposition without having to perform the large number of experiments required by the full factorial design. The correlations between deposition parameters and the output functions have been discussed and presented in the first part of this paper. This is followed, in the second part of this investigation, by an assessment of the feasibility of producing low coercivity iron films.

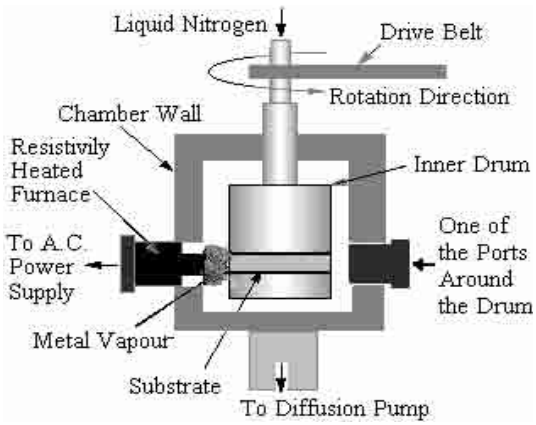

Fig. 1. A schematic of the vertical cross-section through the main body of the RC system.

2 Experimental method

The thin iron films were deposited from iron vapour on to a polyimide (kapton^{TM}) substrate. The substrate was

[a] e-mail: hkockar@balikesir.edu.tr
or hakankockar@hotmail.com
[b] e-mail: meydan@cf.ac.uk

Table 1. The input parameters and level settings used for evaporating thin iron films. Furnace shape is denoted as [width × length] mm^2.

	Input parameters			
Level setting 3	Furnace shape (mm^2)	Mass of material (mg)	Furnace power (watt)	Gap (mm)
1	4×4	060	330	20
2	2×4	090	355	24
3	4×2	120	380	28

attached to the drum of the RC which was filled with liquid nitrogen and rotated at 1300 rpm during deposition. Iron powder (99.0% pure, 1 to 450 micron in diameter) was vaporised from a resistively heated tungsten furnace which was placed in one of the ports around the RC. The deposition time was half an hour for each experiment. The structural analysis of the films was done using X-ray diffraction which concluded that the films have a bcc α-iron crystalline structure.

The orthogonal design is based on studying the relationship between input parameters and their corresponding output functions by selecting certain representative combinations of the input parameter level settings. These level settings fit into certain orthogonal tables [2]. The maximum amount of information can be gained using the least number of experiments, by following the orthogonal tables. In the case of 4 factors at 3 levels, only 9 experimental runs are required, instead of 81 runs needed to achieve the optimised condition in the full multidimensional space [3]. The theory and application of orthogonal design technique are outside the scope of this paper and can be found in detailed elsewhere [4]. It has broad application areas such as; optimisation of thin film deposition equipment, plasma etching, photoresist processing, and optical stepper development.

3 Results and discussion

3.1 Optimisation of input parameters with the output functions of the RC system

In the RC system, it is possible to vary the furnace shape, the mass of the iron powder, the power of furnace, and the gap between substrate and source. Therefore, these four variables serve as our input parameters. Starting with a baseline process using (2 mm wide × 4 mm long) furnace shape, 90 mg of iron powder, 355 watt furnace power, and 24 mm gap between the furnace and the substrate, a level variation using one higher and one lower level was selected, yielding 3 level settings for each input parameter. The level settings and input parameters chosen are shown in Table 1.

The output functions are thickness uniformity across the film and deposition rate. The thickness uniformity is expressed as a percentage and is given by $((x/\text{total width of film}) \times 100\%)$, where x refers to film width at which the thickness varies within ±5%. In the case of run 5, $x = 6.14$ mm, therefore the thickness uniformity $= (6.14/20) \times 100$, which is 30.7%. The deposition rate was calculated from the average thickness value divided by run-time. For example, for run 5, the deposition rate is 0.120 nm/s. In the experimental set-up, four input parameters, each of them with three level settings, fit the orthogonal matrix $L_9 3^4$ [5,6].

Table 2 shows that the results for each of the 9 experiments required by the $L_9 3^4$ matrix are listed, plus two extra experiments labelled $1'$ and $1''$. These experiments are the repeats of the first experiment and give a useful gauge of the random variation in the process.

For example, run 1 in Table 2, the conditions chosen were level setting 1 for each of the input parameters, (4×4) mm^2 furnace shape, 60 mg iron, 330 watt furnace power, and 20 mm gap. These conditions resulted in a thickness uniformity of 13.9% and a deposition rate of 0.057 nm/s in Table 2. Similarly, the data for each of the other experimental conditions in Table 2 and the corresponding results in Table 4 are listed.

Using the formulae in Table 3, the first order data analysis, which is sufficient in the vast majority of process optimisation and characterisation work, has been done as follows: the output function average (arithmetic means) for each level setting and for each input parameter are determined and listed in Table 4. Therefore, the thickness uniformity average for (4×4) mm^2 furnace shape setting 1 (runs 1, 2, and 3) is given by the average of $U_1(28.4\%)$, $U_2(44.3\%)$, and $U_3(31.7\%)$. This is denoted as U_{s_1} and is 34.8%. The average of the same three runs $[U_1(13.9\%), U_{1'}(38.1\%)\, U_{1''}(33.2\%)]$ is taken as $U_1(28.4\%)$ for run 1. Similarly, the thickness uniformity average for furnace shape setting 2, (2×4) mm^2, is given by the average of the thickness uniformity for the experiments 4, 5 and 6 and is $U_{s_2} = 33.0\%$. The thickness uniformity average for furnace shape setting 3 is $U_{s_3} = 23.4\%$.

As can be seen in Table 4, the first order effect of changing the furnace shape (4×4) mm^2, (2×4) mm^2, and (4×2) mm^2 is to decrease the thickness uniformity from 34.8%, 33.0% and finally to 23.4%, respectively. Using the formulae given in Table 3, the output function averages for each of the input parameter levels can be calculated for the thickness uniformity and the deposition rate. This has function averages (ΔU, ΔD). The thickness uniformity difference for furnace shape, ΔU_s, is $U_{s_1} - U_{s_3}$, or 11.4%. Similarly the thickness uniformity difference for mass is given by $\Delta U_m = U_{m_3} - U_{m_1}$ or 15.3%. In our case, it can be seen that the largest difference for the thickness uniformity (ΔU_g) is 20.7% that is due to the gap between the substrate and furnace. The calculated values of the output function differences are shown in Table 4. By comparing the four differences, it is possible to quantify the relative effect of each input parameter on thickness uniformity over the level setting range chosen for that parameter. It should be emphasised that this approach to data analysis is the simplest approach; more sophisticated statistical approaches can be found elsewhere (6,7).

Table 2. The orthogonal experimental results for thickness uniformity (%) and deposition rate (nm/s).

	Input parameters				Output functions	
Run	Furnace shape (mm^2)	Mass (mg)	Power (watt)	Gap (mm)	Thickness uniformity (%)	Deposition rate(nm/s)
1	(1) 4×4	(1) 060	(1) 330	(1) 20	$U_1 = 13.9$	$D_1 = 0.057$
2	(1) 4×4	(2) 090	(2) 355	(2) 24	$U_2 = 44.3$	$D_2 = 0.013$
3	(1) 4×4	(3) 120	(3) 380	(3) 28	$U_3 = 31.7$	$D_3 = 0.075$
4	(2) 2×4	(1) 060	(2) 355	(3) 28	$U_4 = 12.9$	$D_4 = 0.010$
5	(2) 2×4	(2) 090	(3) 380	(1) 20	$U_5 = 30.7$	$D_5 = 0.012$
$1'$	(1) 4×4	(1) 060	(1) 330	(1) 20	$U_{1'} = 38.1$	$D_{1'} = 0.052$
6	(2) 2×4	(3) 120	(1) 330	(2) 24	$U_6 = 55.4$	$D_6 = 0.163$
7	(3) 4×2	(1) 060	(3) 380	(2) 24	$U_7 = 25.8$	$D_7 = 0.024$
8	(3) 4×2	(2) 090	(1) 330	(3) 28	$U_8 = 18.8$	$D_8 = 0.094$
9	(3) 4×2	(3) 120	(2) 355	(1) 20	$U_9 = 25.8$	$D_9 = 0.152$
$1''$	(1) 4×4	(1) 060	(1) 330	(1) 20	$U_{1''} = 33.2$	$D_{1''} = 0.077$

Table 3. Formulae for output function averages and output function differences for the orthogonal table $L_9 3^4$. (The subscripts used are: s for furnace shape, m for mass, p for furnace power, g for gap between the substrate and resistively heated furnace.)

$U_{s_1} = 1/3(U_1 + U_2 + U_3)$	$U_{m_1} = 1/3(U_1 + U_4 + U_7)$
$U_{s_2} = 1/3(U_4 + U_5 + U_6)$	$U_{m_2} = 1/3(U_2 + U_5 + U_8)$
$U_{s_3} = 1/3(U_7 + U_8 + U_9)$	$U_{m_3} = 1/3(U_3 + U_6 + U_9)$
$\Delta U_s = U_s(\max.) - U_s(\min.)$	$\Delta U_m = U_m(\max.) - U_m(\min.)$
$U_{p_1} = 1/3(U_1 + U_6 + U_8)$	$U_{g_1} = 1/3(U_1 + U_5 + U_9)$
$U_{p_2} = 1/3(U_2 + U_4 + U_9)$	$U_{g_2} = 1/3(U_2 + U_6 + U_7)$
$U_{p_3} = 1/3(U_3 + U_5 + U_7)$	$U_{g_3} = 1/3(U_3 + U_4 + U_8)$
$\Delta U_p = U_p(\max.) - U_p(\min.)$	$\Delta U_g = U_g(\max.) - U_g(\min.)$

Table 4. The corresponding analysis of Table 3 for output function averages and output function differences, and standard deviations.

Analysis of the results					
Run	F. shape (mm^2)	Mass (mg)	Power (watt)	Gap (mm)	Standard deviations
U_1	$U_{s_1} = 34.8$	$U_{m_1} = 22.3$	$U_{p_1} = 34.2$	$U_{g_1} = 28.3$	
U_2	$U_{s_2} = 33.0$	$U_{m_2} = 31.3$	$U_{p_2} = 27.6$	$U_{g_2} = 41.8$	
U_3	$U_{s_3} = 23.4$	$U_{m_3} = 37.6$	$U_{p_3} = 29.4$	$U_{g_3} = 21.1$	
ΔU	$\Delta U_s = 11.4$	$\Delta U_m = 15.3$	$\Delta U_p = 7.2$	$\Delta U_g = 20.7$	Std $Dev_U = 12.8$
D_1	$D_{s_1} = 0.05$	$D_{m_1} = 0.03$	$D_{p_1} = 0.11$	$D_{g_1} = 0.11$	
D_2	$D_{s_2} = 0.10$	$D_{m_2} = 0.08$	$D_{p_2} = 0.06$	$D_{g_2} = 0.07$	
D_3	$D_{s_3} = 0.09$	$D_{m_3} = 0.13$	$D_{p_3} = 0.07$	$D_{g_3} = 0.06$	
ΔD	$\Delta D_s = 0.05$	$\Delta D_m = 0.10$	$\Delta D_p = 0.07$	$\Delta D_g = 0.05$	Std $Dev_D = 0.01$

It is now easy to determine a process that will yield the highest thickness uniformity. Table 4 shows that the maximum thickness uniformity for each input parameter occur for the (4×4) mm^2 furnace shape, the largest amount of material, the lowest power and a gap of 24 mm. The process is optimised for maximum thickness uniformity at these level settings. This recipe, represented by level settings 1, 3, 1, 2 for furnace shape, mass, power, and gap respectively, is not one of the experiments included in the original $L_9 3^4$ orthogonal matrix. Going back to the RC system and running this recipe is expected to give a higher thickness uniformity than any of the thickness uniformities obtained in the 9 original experiments. However, in this case, the output function differences for furnace shape and furnace power is less than the standard deviation of the thickness uniformity, which means the furnace shape and the power do not affect thickness uniformity greatly therefore only the mass and gap have an effect on it.

Furthermore, in practice, due to the limitation of the RC system it cannot exceed those values used in the experimental system for the input parameters. For example, in the case of furnace power, 330 watt represents the

Table 5. The orthogonal experimental results for coercivity (top), and the corresponding analysis (bottom).

	Input parameters				Output function
Run	Furnace shape (mm)	Mass (mg)	Power (watt)	Gap (mm)	Coercivity H_c (kA/m)
1	(1) 4×4	(1) 060	(1) 330	(1) 20	$C_1 = 03.78$
2	(1) 4×4	(2) 090	(2) 355	(2) 24	$C_2 = 16.90$
3	(1) 4×4	(3) 120	(3) 380	(3) 28	$C_3 = 05.45$
4	(2) 2×4	(1) 060	(2) 355	(3) 28	$C_4 = 12.80$
5	(2) 2×4	(2) 090	(3) 380	(1) 20	$C_5 = 04.60$
$1'$	(1) 4×4	(1) 060	(1) 330	(1) 20	$C_{1'} = 11.80$
6	(2) 2×4	(3) 120	(1) 330	(2) 24	$C_6 = 07.40$
7	(3) 4×2	(1) 060	(3) 380	(2) 24	$C_7 = 14.40$
8	(3) 4×2	(2) 090	(1) 330	(3) 28	$C_8 = 10.80$
9	(3) 4×2	(3) 120	(2) 355	(1) 20	$C_9 = 03.20$
$1''$	(1) 4×4	(1) 060	(1) 330	(1) 20	$C_{1''} = 06.10$
C_1	$C_{s_1} = 09.86$	$C_{m_1} = 11.48$	$C_{p_1} = 08.48$	$C_{g_1} = 05.01$	
C_2	$C_{s_2} = 08.27$	$C_{m_2} = 10.77$	$C_{p_2} = 10.97$	$C_{g_2} = 12.90$	
C_3	$C_{s_3} = 09.47$	$C_{m_3} = 05.35$	$C_{p_3} = 08.15$	$C_{g_3} = 09.68$	
C_s	$\Delta C_s = 01.59$	$\Delta C_m = 06.13$	$\Delta C_p = 02.82$	$\Delta C_g = 07.89$	Std. $\text{Dev}_C = 04.50$

optimised furnace power settings, and a greater rate could be achieved by going to a power of more than 380 watt however this would melt the pouch.

Finally, the redundant experimental runs, 1, $1'$ and $1''$, can be used to calculate the standard deviation. The relative significance of the output function averages can then be determined by comparison to the standard deviation.

In this work, the thickness uniformity has been the sole subject of the discussion, but the deposition rate is also important in developing an optimal process. In examining the averages and differences for thickness uniformity and deposition rate shown in Table 4, with the goal of having the best thickness uniformity and fastest deposition rate, the following recipe would be chosen, as 1, 3, 1, 2 and 2, 3, 1, 1 respectively.

The best thickness uniformity is gained at furnace shape level 1, while the fastest rate is at furnace shape level 2. However, the effect of furnace shape on thickness uniformity is less than the standard deviation (see Tab. 4), therefore not significant over the furnace shape studied. Thus optimum process can operate at furnace shape setting 2, resulting in the best deposition rate with no impact on thickness uniformity. Even though the effect of mass on thickness uniformity is almost equivalent to the standard deviation and the effect of power is less than the standard deviation, the best deposition rate for mass is 3 and for power is 1. The gap setting is chosen by again comparing the strengths of the output function averages, and the differences of the output function compared to the standard deviation. Gap has almost the same effect on thickness uniformity and on deposition rate, but for the application of thin iron film, it is important to have the more uniform thickness in film than the faster deposition rate. Therefore, the optimum output parameters would be: 2, 3, 1, 2.

The subsequent thickness uniformity and deposition rate results derived using this recipe are 40.1% and 0.424 nm/s. These results are a substantial improvement over the results seen in the eleven experimental runs required by the orthogonal matrix.

3.2 The effect of deposition in producing low coercivity iron films

The same four input parameters with 3 level settings for each input parameter are shown in Table 1. The coercivity, H_c (kA/m) of the thin iron films and measured by a vibrating sample magnetometer (VSM) is the output function. Table 5 shows the input parameters and output functions together with analysis of the results for each of the 9 experiments required by the $L_9 3^4$ matrix together with two extra experiments labelled $1'$ and $1''$.

The conditions chosen for run 1 were level setting 1 for each of the input parameters, (4×4) mm furnace shape, 60 mg iron, 330 watt furnace power, and 20 mm gap. These conditions resulted in a coercivity value of 3.78 kA/m. Similarly, the data for each of the other experimental conditions and the corresponding results are listed in Table 5.

Using the first order data analysis, the output function average for each level setting and for each input parameter are determined. The coercivity average for (4×4) mm furnace shape setting 1 (runs 1, 2, and 3) is given by the average of $C_1(7.23)$, $C_2(16.90)$, and $C_3(5.45)$. This is denoted as C_{s_1} and is 9.86. The average of the same three runs [$C_1(13.9)$, $C_{1'}(38.1)$, and $C_{1''}(33.2\%)$] is taken as $C_1(7.23)$ for run 1. Similarly, the coercivity average for furnace shape setting 2, (2×4) mm, is given by the average of the coercivity for the experiments 4, 5, and 6 and is $C_{s_2} = 8.27$. The coercivity average for furnace shape setting 3 is $C_{s_3} = 9.47$. The first order effect of changing the furnace shape to (4×4) mm, (2×4) mm, and (4×2) mm is to change the coercivity to 9.86, 8.27 and 9.47 respectively.

The coercivity difference for furnace shape, ΔC_s, is $C_{s_1} - C_{s_2} = 1.59$. Similarly the coercivity difference for mass is given by $\Delta C_m = C_{m_1} - C_{m_3} = 6.13$. The largest difference for coercivity (ΔC_g) is 7.89 that is due to the gap spacing. By comparing the four differences, it is possible to quantify the relative effect of each input parameter on coercivity over the level setting range chosen for that parameter.

Table 5 shows that the low coercivity for each input parameter occur at the (2×4) mm furnace shape, the largest amount of material, the highest power, and the smallest gap. The process is optimised at these level settings with the goal of attaining an iron film with the lowest coercivity. The lowest coercivity is gained at furnace shape level 2. However, the effect of furnace shape on coercivity is less than the standard deviation, therefore not significant for the furnace shapes studied. Even though the optimum process can operate at any of the furnace shape settings, it would be logical to chose the level setting 2. The effect of mass on coercivity is slightly bigger than the standard deviation and the effect of power is less than the standard deviation, the lowest coercivity for mass is 3 and for power is 3. The gap setting is chosen by again comparing the strengths of the output function averages, and the differences of the output function compared to the standard deviation. The gap has the biggest influence on coercivity, the obvious choice is setting 1. Therefore, the optimum output parameters for reducing coercivity would be 2, 3, 3, and 1 for furnace shape, mass, power, and gap respectively. This configuration is not one of the experiments included in the original $L_9 3^4$ orthogonal matrix.

The subsequent coercivity derived using this recipe is 1.2 kA/m. This result is an improvement over the results seen in the eleven experimental runs required by the orthogonal matrix. By comparing the output function differences (ΔC_s, ΔC_m, ΔC_p, and ΔC_g) with standard deviation for coercivity, only the mass and gap is expected to have an influence on the coercivity. Further information can be gained from the orthogonal matrix by plotting the level averages as a function of level setting in Figure 2. As seen in Figure 2, if the level settings are extended beyond the chosen for original matrix, it should be possible to achieve even lower coercivity. In practise, due to the limitation of the RC system it cannot exceed those values used in the experimental system.

Furnace Shape (mm)	Cs (kA/m)
4*4	9.86
2*4	8.27
4*2	9.47

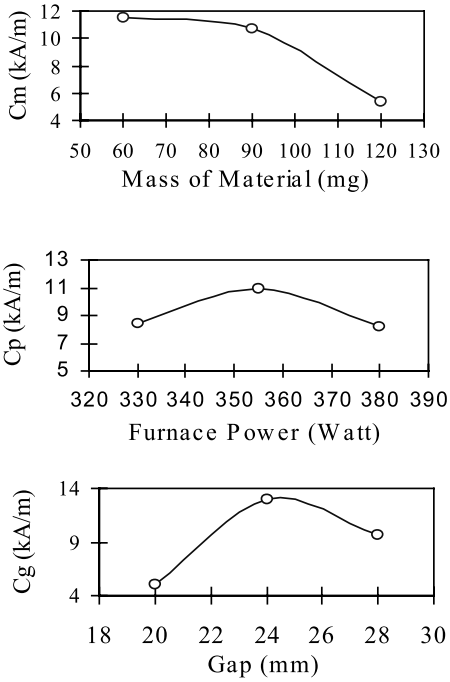

Fig. 2. A plot of the output function averages from Table 5 as a function of the input parameter level settings.

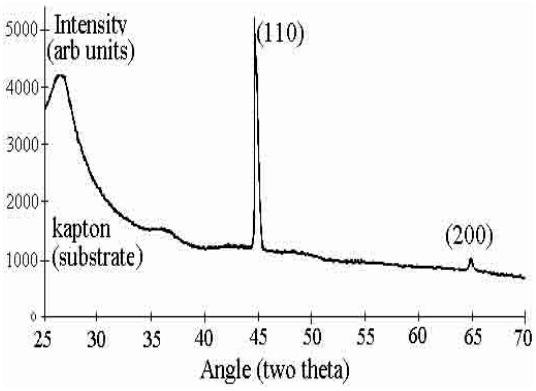

Fig. 3. Typical X-ray diffraction traces showing the bcc α-iron structure of iron film evaporated by the RC system.

3.3 Structural analysis

The structural characteristic of the films was determined using XRD. The X-ray measurements were made with Cu Kα radiation in the range of $25° < 2\theta < 70°$, where θ is the Bragg angle. Bragg reflections were obtained for $2\theta = 45°$, $65°$ as shown in Figure 3 which correspond to the (110) and (200) reflections of the body-centred cubic (bcc) structure of α-iron. Transmission electron microscopy measurements also confirmed that the films have a polycrystalline structure.

4 Conclusions

The magnetic material has been produced by a novel RC technique, and its optimisation for magnetic material production together with the low coercivity iron film production was systematically investigated by using a orthogonal design technique.

The results of orthogonal analysis indicate that the thickness uniformity across the film was not improved, due to the large standard deviation, but the optimum deposition rate was obtained, by using the chosen control parameters. The reason for this is simply that the relatively small dimensions of the RC system imposes limitations on its operation when depositing magnetic films *i.e.*, the limited space inside the vacuum chamber makes it difficult to vary gap between substrate and the evaporation source.

For the purpose of developing low coercivity iron film the orthogonal process technique was applied. The results of orthogonal analysis indicate that there is no effect of the furnace shape, and power on coercivity, and only a small effect on coercivity due the mass and the gap, however the process was optimised to reduce the coercivity by using the chosen control parameters. The large standard deviations over the optimised measurements are thought to be in part due to the difficulty in maintaining consistent deposition conditions.

A continuation of this work therefore requires a new system that incorporates the novel features of the present RC system but without its limitations.

The grant of Celal Bayar University, Turkey for H. Kockar is acknowledged for the major part of this investigation in Cardiff University, Wolfson Centre, UK.

References

1. J.A. Howard, B. Mile, Acc. Chem. Res. **20**, 173 (1987).
2. W.G. Cochran, G.M. Cox, *Experimental Design* (John Wiley & Sons, NY, 1957).
3. O. Kempthorn, *The Design and Analysis of Experiments* (R.E. Krieger Publishing Co., Huntington, NY, 1979).
4. G. Taguchi, *Experimental Designs*, 3rd edn. (Maruzen Publishing Co., Tokyo, Japan, 1977), Vol. 2.
5. R.N. Kackar, J. Quality Technol. **17**, 176 (1985).
6. D. Raghavarao, *Construction and Combinatorial Problems in Design of Experiments* (John Wiley & Sons, NY, 1971).
7. W.J. Diamond, *Practical Experiment Designs* (Van Nostrand Reinhold Co., NY, 1981).